MATERIAL CHARACTERISTICS OF SMALL-SEED CROPS: MILLET, BROOMCORN MILLET, AND RAPESEED

/

谷子、糜子和油菜籽小籽粒种子的物料特性研究

Zhiwei WANG[1)], Jianguo ZHOU[1)], Naishuo WEI[1)], Deyi ZHANG[1)], Sugirbay ADILET[2)], Yanwu JIANG[1)], Jun CHEN[1*)]

[1)] College of Mechanical and Electronic Engineering, Northwest A&F University, Yangling, Shaanxi, 712100, China

[2)] Research School of Veterinary Medicine and Agriculture, Shakarim University, Semey 071400, Kazakhstan

** Corresponding author: Jun Chen. E-mail address: chenjun_jdxy@nwsuaf.edu.cn*

DOI: https://doi.org/10.35633/inmateh-78-84

Keywords: *Small-seed crops, Pneumatic seed metering device, Friction coefficient, Elastic modulus, Poisson's ratio, Coefficient of restitution*

ABSTRACT

To provide fundamental data for the design and experimental evaluation of pneumatic precision seed metering devices for small-seed crops, the material characteristics of millet, broomcorn millet, and rapeseed were systematically investigated in this study. The moisture content, thousand-seed weight, density, principal dimensions, equivalent diameter, and angle of repose of the three seed types were determined through physical measurements. The Poisson's ratios of millet, broomcorn millet, and rapeseed were measured using a universal testing machine and were found to be 0.27, 0.33, and 0.29, respectively. In addition, the static and dynamic friction coefficients between each seed type and acrylic, stainless steel, and resin surfaces were obtained. The elastic moduli of millet, broomcorn millet, and rapeseed were measured using a texture analyzer as 351.76, 589.14, and 133.37 MPa, respectively, which were closely related to seed density and structural characteristics. To further clarify the influence of seed–surface collision behavior on seed motion trajectories during the seed metering process, a high-speed imaging test system was established to determine the coefficients of restitution of seeds with moisture contents of 15%, 20%, and 25% after collision with different material surfaces. The results showed that the coefficient of restitution was significantly affected by seed moisture content and decreased markedly with increasing moisture content. Among the three seed types, the coefficient of restitution decreased in the order of broomcorn millet, millet, and rapeseed. For each seed type, the coefficient of restitution decreased sequentially for collisions with acrylic, stainless steel, resin, and the corresponding seed surface. These results provide important data support for the structural design and simulation analysis of pneumatic precision seed metering devices.

摘要

为给小籽粒气力式排种器的设计与试验提供数据支撑，本文选取谷子、糜子和油菜籽对其物料特性进行了系统研究。通过测量试验得到了三种种子的含水率、千粒重、密度、三轴尺寸、等效直径、自然休止角等具体参数数值。利用万能试验机得到三类种子的泊松比分别为0.27,0.33 和0.29。得到了三类种子分别与亚克力板、不锈钢板和树脂板之间的动、静摩擦系数。使用质构仪得到三类种子的弹性模量分别为 351.76MPa、589.14MPa 和133.37MPa，这与种子的密度和构造有对应的关系。为分析种子与排种器接触过程中碰撞行为对其运动轨迹的影响，搭建了高速摄像测试系统，测定了15%、20%、25%不同含水率种子与不同材料接触后的碰撞恢复系数。结果表明：碰撞恢复系数与含水率有显著关系，随着含水率的增加，碰撞恢复系数迅速减小；糜子、谷子、油菜籽的碰撞恢复系数依次减小；每类种子与亚克力板、不锈钢板、树脂板、同类种子板之间的碰撞恢复系数依次减小。该研究可为小籽粒气吸式排种器的结构设计与仿真分析提供重要的数据支撑。

INTRODUCTION

Small-seed crops, such as millet, broomcorn millet, and rapeseed, are widely cultivated in China and play an important role in regional agricultural production, especially in Northwest China *(Li et al., 2023c)*. In practical production, precision seeding has gradually become an important technical approach for improving seed-use efficiency, emergence uniformity, and field productivity *(Onal et al., 2012; St Jack et al., 2013; Jin et al., 2019; Dun et al., 2025)*.

Among the key components of precision seeders, the pneumatic seed metering device has attracted increasing attention because of its strong adaptability, good singulation potential, and suitability for small seeds *(Singh et al., 2005; Ibrahim et al., 2018; Li et al., 2023a)*. In recent years, many studies have focused on the structural design, airflow characteristics, and operating performance of pneumatic seed-metering systems for rapeseed, vegetables, and other small-seed crops *(Yang et al., 2016; Yuan et al., 2022; Li et al., 2023b; Zhang et al., 2025)*. Existing research has shown that the performance of pneumatic seed metering is closely related to seed suction stability, seed motion behavior, and seed–device interaction during filling, transport, and release *(Yazgi et al., 2014; Xu et al., 2022)*. However, although structural optimization and numerical simulation of seed metering devices have been extensively studied, the supporting material-property data of small-seed crops are still insufficient in many cases.

For the design, optimization, and numerical simulation of pneumatic seed metering devices, accurate seed material parameters are indispensable *(Karayel, 2009; Sun et al., 2017)*. Parameters such as seed size, density, angle of repose, static and kinetic friction coefficients, Poisson's ratio, elastic modulus, shear modulus, and coefficient of restitution directly affect seed suction behavior, seed–wall interaction, collision response, and particle motion in the seed-metering process *(Karayel et al., 2004; Lai et al., 2020; Lai et al., 2023; Li et al., 2025)*. In particular, these parameters are essential for contact-model establishment, parameter calibration, and reliability improvement in DEM simulation, CFD-DEM coupling, and engineering design of seed-metering components *(Hu et al., 2021; Lei et al., 2021; Liu et al., 2022)*. Nevertheless, for representative small-seed crops such as millet, broomcorn millet, and rapeseed, systematic and comparative studies on these material characteristics are still limited, and the available data are often scattered, incomplete, or obtained under different test conditions.

Accordingly, this study selected millet, broomcorn millet, and rapeseed as representative small-seed crops and systematically investigated their basic physical and mechanical characteristics. The main objectives were:

(1) to determine the basic physical parameters of the three seed types, including moisture content, thousand-seed weight, density, three-axis dimensions, equivalent diameter, and angle of repose;

(2) to measure their interaction characteristics with common contact materials used in seed metering devices, including static and kinetic friction coefficients;

(3) to determine key mechanical parameters required for engineering design and simulation, including Poisson's ratio, elastic modulus, and shear modulus; and

(4) to evaluate the coefficient of restitution of the seeds under different moisture contents, drop heights, and contact materials using a high-speed imaging system.

The results of this study provide essential parameter support for the design, simulation, and optimization of pneumatic precision seed metering devices for small-seed crops, and also offer a material-property basis for improving seed-motion analysis and engineering application of multi-seed-per-hill precision seeding technology.

MATERIAL AND METHODS

Experimental materials

Three representative small-seed crops—millet, broomcorn millet, and rapeseed—were selected for the experiments. The seed varieties used were Yugu 181 (Handan, Hebei; Hebei Yike Seed Industry Co., Ltd.), Dahuangmi (Harbin, Heilongjiang; Harbin Jinlong Agricultural Co., Ltd.), and Wuyue Man (Cangzhou, Hebei; Cangzhou Jinke Lifeng Seedling Co., Ltd.).

Due to the presence of impurities, particularly in millet, the seeds were first cleaned using an electric blower (Kemaisi, China) to remove dust, seed coats, and other impurities. Since seed size is one of the key factors affecting suction stability and the probability of multiple-seed adsorption at a single suction hole, size grading was performed before the experiments to reduce the influence of undersized and shriveled seeds. Subsequently, a fan and custom sieves with round-hole diameters of 1.3, 1.5, 1.7, 2.3, and 2.5 mm were used for further cleaning and size grading. Shriveled and underfilled seeds were removed during this process.

As shown in Table 1, the length, width, and thickness of the seeds were measured to calculate their equivalent diameters. Based on the approximately normal distribution of these dimensions, the seeds were classified into small, medium, and large size groups. Low-quality seeds in the small-size group were discarded. Seeds with equivalent diameters greater than 1.500 mm for millet, 2.300 mm for broomcorn millet, and 1.900 mm for rapeseed were selected for subsequent experiments.

Table 1

Seeds grading criteria

Seed type	Small diameter [mm]	Medium diameter [mm]	Large diameter [mm]
Millet	Min-1.500	1.500-1.700	1.700-max
Broomcorn millet	Min-2.300	2.300-2.500	2.500-max
Rapeseed	Min-1.900	1.900-2.100	2.100-max

Experimental instruments and equipment

The main instruments and equipment used in this study are listed in Table 2. These instruments were employed to measure key parameters of the selected small-seed varieties, including moisture content, thousand-seed weight, density, three-axis dimensions, angle of repose, and static and kinetic friction coefficients.

In addition, the coefficient of restitution, Poisson's ratio, elastic modulus, and shear modulus were experimentally determined. Table 2 also summarizes the corresponding test items and applications of each instrument.

Table 2

Main instruments and equipment used in the experiments

Instrument	Manufacturer and model	Accuracy and range	Measurement purpose
Digital vernier caliper	Greener	0.01 mm; [0-300.00mm]	Seed length, width, and thickness
Electronic balance	Goloni Industrial	0.01 g; [0-1000.00g]	Seed weight measurement
Graduated cylinder	500 mL	1.0 mL; [0-500.0mL]	Seed volume
Vacuum drying oven	Supor DZF6050	-	Seed drying
High-speed camera	Olympus I-speed TR	300fps	Seed motion analysis
Laptop computer	Mechanic F117	-	Data acquisition and processing
Sieve	Yuanzhi Machinery Co., Ningjing	0.1mm; [0.5-5mm]	Seed size grading
Inclinometer	Self-made	1°; [0-60°]	Kinetic and static friction coefficients
Electronic angle gauge	Greener	0.01°; [0-180°]	Angle measurement
Moisture meter	Huachao HC3	0.01%; [0.01-99.99%]	Seed moisture content
Food grinder	China Shuangqiang	[0-500 mL]	Seed grinding
Universal testing machine	Changchun DDL10, China	±0.5%	Seed Poisson's ratio
Texture analyzer	FTC Texture Analyzer TMS-PRO, USA	±0.5%	Seed elastic modulus
Dust remover	Comess GFJ Blower	1.0m/s; [1.0-10.0m/s]	Seed cleaning

Basic seed parameters

For each seed type, 1,000 seeds were counted, placed in a paper container, and weighed using an electronic balance. The thousand-seed weight was calculated by subtracting the container mass from the total mass. Five replicates were performed for each seed type, and the average value was used as the final result *(Zhang et al., 2025)*.

Seed density was determined in accordance with *GB/T 5518-2008 (Grain and Oil Inspection—Determination of Relative Density of Grains and Oilseeds)* using the water displacement method with distilled water. Each measurement was repeated five times, and the average value was taken as the final density *(Yuan et al., 2022)*.

In the design of seed metering devices, three mutually perpendicular axial dimensions—length, width, and thickness—are commonly used. The length refers to the maximum dimension in the seed's planar projection, the width refers to the maximum dimension perpendicular to the length, and the thickness is the linear dimension perpendicular to both the length and width. The equivalent diameter of a seed can be calculated using the following formula:

$$D = \sqrt[3]{L \cdot W \cdot T} \quad (1)$$

where:

D - the seed equivalent diameter, mm; L - the seed length, mm; W - the seed width, mm; T - the seed thickness, mm.

A random selection of 100 seeds each of millet, broomcorn millet, and rapeseed was made. The three axial dimensions of each seed—length, width, and thickness—were measured using a vernier caliper with a precision of 0.01 mm. The measured data for the 100 seeds of each type were then substituted into Equation (1) to calculate the equivalent diameter of the seeds.

The angle of repose was measured using the discharge method. A funnel with an outlet diameter of 2 cm and a cone angle of 120° was used. The funnel was first placed on a smooth horizontal surface and filled with seeds. It was then lifted vertically to allow the seeds to flow freely and form a pile. The angle of repose was measured using an electronic angle gauge. Each test was repeated five times, and the average value was recorded.

Seed moisture content (wet basis) was determined according to *GB/T 3543.6-1995 (Crop Seed Testing Procedures: Determination of Moisture Content)* using the oven-drying method. The seeds were first ground, then dried in a vacuum oven at 70 °C for 12 h. Each seed type was tested in five replicates, and the mean value was used.

To investigate the effect of moisture content on the coefficient of restitution, seeds with target moisture contents of 15%, 20%, and 25% were prepared. The required amount of distilled water was added to the seeds, which were then sealed and allowed to equilibrate until the desired moisture content was achieved, as calculated using Equation (2). The target moisture content was adjusted on a wet basis according to the principle of dry matter conservation.

$$w_2 = \frac{w_1 \cdot m_1 + m_2}{m_1 + m_2} \times 100\% \quad (2)$$

where:

w_1 - seed moisture content on wet basis, %; w_2 - final seed moisture content on wet basis, %;

m_1 - mass of seeds after drying, g; m_2 - initial mass of seeds, g.

Static friction coefficient and kinetic friction coefficient

The contact surfaces of seed metering devices are typically made of acrylic, stainless steel, or resin. To investigate the interaction between seeds and these materials, the static and kinetic friction coefficients were measured. Accordingly, acrylic, stainless steel, and resin plates were selected as representative contact materials. The density, elastic modulus, and Poisson's ratio of these materials are listed in Table 3 *(Yang et al., 2016)*.

Table 3

Mechanical characteristics of contact materials

Materials	Density [kg/m³]	Elastic modulus [Mpa]	Poisson's ratio
Acrylic plate	1180	2350	0.364
Stainless steel plate	7900	206000	0.270
Transparent resin plate	1117	3200	0.370

The friction coefficients were determined using the inclined plane method *(Li et al., 2025)*. Cleaned seeds of three types at different moisture contents were fixed onto transparent adhesive tape (width: 5 cm) to prepare seed plates. For each seed type, five plates with a length of at least 5 cm were prepared.

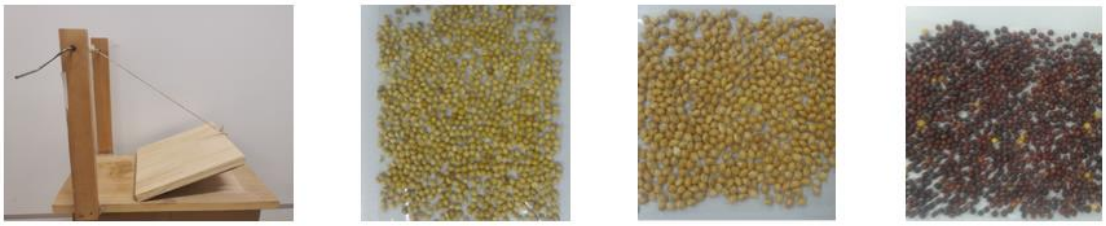

Fig. 1 - Inclined plane test for friction coefficient measurement

(a) Inclined plane apparatus; (b) Millet seed plate; (c) Broomcorn millet seed plate; (d) Rapeseed seed plate

A self-designed inclined plane apparatus was used, as shown in Fig. 1. Before testing, the platform was leveled to ensure horizontal alignment. The selected material plates (acrylic, stainless steel, and resin) were fixed on the inclined surface, and friction tests were conducted using seed plates of millet, broomcorn millet, and rapeseed.

During the test, the seed plate was placed on the inclined surface, and the inclination angle was gradually increased by rotating the handle at a low speed. When the seed plate began to slide, the rotation was stopped immediately, and the corresponding angle was recorded using an electronic inclinometer. For each seed type and moisture level, five replicates were conducted, and the average value was used. The static friction coefficient was calculated using Equation (3).

$$\mu_s = \frac{F_f}{F_N} = \frac{mg\sin\alpha}{mg\cos\alpha} = \tan\alpha \tag{3}$$

where:

μ_s - the static friction coefficient of the seeds; F_f - the maximum static friction force between two contact surfaces, N; F_N - Positive pressure of the material to be tested on the seeds, N; α - the inclination angle of the slope when seed begins to slide down on it, °.

The same method was used to determine the kinetic friction coefficient. The inclination angle was increased until the seeds started to move continuously along the surface. The kinetic friction coefficient was calculated based on the corresponding critical angle and denoted as μ_k.

$$\mu_k = \tan\theta \tag{4}$$

where:

θ - the inclination angle of a slope when seed slides uniformly on it, °.

Poisson's Ratio

Fig. 2 shows the experimental setup used to determine the Poisson's ratio of seeds using a universal testing machine. Three types of seeds were tested, with 10 samples selected for each group.

An electronic universal testing machine was used to apply a compressive load along the longitudinal direction (*L*) of the seed at a loading rate of 0.01 mm/s. The loading process was stopped when initial signs of rupture appeared, and the deformation in the longitudinal direction was recorded. Simultaneously, the transverse deformation (width direction) was measured using a vernier caliper *(Sun et al., 2017; Li et al., 2023)*.

The Poisson's ratio Δ was calculated using Equation (5).

$$\Delta = -\frac{\varepsilon'}{\varepsilon} = \frac{(b - B')/B'}{(L' - l)/L'} \tag{5}$$

where:

Δ - Poisson's ratio of the seed; ε'- the strain in the width direction; ε - the strain in the length direction; L'- the initial seed length before loading, mm; l - the seed length at the point of rupture, mm; B'- the initial seed width before loading, mm; b- the seed width at the point of rupture, mm.

(a) (b)

Fig. 2 - Compression test for Poisson's ratio measurement

(a) Universal testing system; (b) Seed compression test

Elastic modulus and shear modulus

The elastic modulus characterizes the resistance of a material to elastic deformation. A higher elastic modulus indicates greater stiffness and lower deformability, whereas a lower modulus corresponds to easier deformation under load *(Sun et al., 2017; Liu et al., 2022; Li et al., 2025)*.

The elastic modulus of seeds was determined using a compression method, as illustrated in Fig. 3(a). In this method, a seed is placed between two parallel plates, and a gradually increasing compressive load is applied. The corresponding force–displacement curve is recorded.

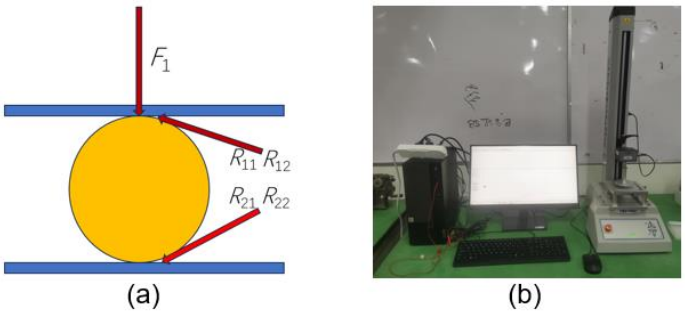

(a) (b)

Fig. 3 - Compression test for elastic modulus measurement

(a) Measurement principle; (b) Experimental setup

The elastic modulus (E) of the seed can be expressed as:

$$E = \frac{0.531F_1(1-\Delta^2)}{S_1^{3/2}}\left[\left(\frac{1}{R_{11}}+\frac{1}{R_{12}}\right)^{\frac{1}{3}}+\left(\frac{1}{R_{21}}+\frac{1}{R_{22}}\right)^{\frac{1}{3}}\right]^{3/2} \quad (6)$$

where:

E - the elastic modulus of the seed, MPa; F_1 - the applied pressure, N; S_1 - the deformation of the seed due to compression, mm; R_{11}、R_{12} - the radii of curvature of the contact points on the seed's upper surface with the top compression plate, mm; R_{21}、R_{22} - the radii of curvature of the contact points on the seed's lower surface with the top compression plate, mm.

Since the seeds of millet, broomcorn millet, and rapeseed are approximately spherical, to simplify the calculation, we assume that $R_{11}=R_{12}=R_{21}=R_{22}$ and that $L=T=W$. Although the three seed types were not perfect spheres, they were approximated as near-spheroidal particles for simplified estimation of elastic modulus. The validity and limitation of this approximation were assessed by comparing the three-axis dimensions listed in Table 5. Then the formula for the elastic modulus of the seed becomes:

$$\begin{cases} R_{11} = \dfrac{(L/2)^2+(T/2)^2}{T} \\ R_{12} = \dfrac{(W/2)^2+(T/2)^2}{T} \end{cases} \quad (7)$$

By substituting the formula from Equation (7) into Equation (6):

$$E = \frac{2.124F_1(1-\Delta^2)R_{11}^{1/2}}{S_1^{3/2}} \quad (8)$$

As shown in Fig. 3(b), a texture analyzer was used to perform the compression tests. A probe with a maximum load capacity of 500 N was selected. The pre-test speed was set to 0.1 mm/s, the test speed to 0.01 mm/s, and the trigger force to 1 N. After compression, the probe returned at a speed of 1 mm/s. Ten valid measurements were conducted for each seed type, and the average value was used.

The shear modulus of the seeds can be calculated using the following formula:

$$G = \frac{E}{2(1+\Delta)} \tag{9}$$

where: G - shear modulus of seeds, MPa.

Coefficient of restitution

The coefficient of restitution characterizes the ability of a seed to recover from deformation after impact *(Hu et al., 2021; Liu Yang et al., 2022)*. It is a key parameter in the design and simulation of seed metering devices and depends on the characteristics of the contacting materials.

The coefficient of restitution is defined as the ratio of the normal relative separation velocity to the normal relative approach velocity during collision, and can be expressed as:

$$\eta = \frac{v_{22} - v_{12}}{v_{21} - v_{11}} = \frac{\sqrt{2gh_2}}{\sqrt{2gh_1}} = \frac{\sqrt{h_2}}{\sqrt{h_1}} \tag{10}$$

where:

η - the coefficient of restitution of the seed; v_{21}-v_{11} - the relative velocity of the seed and the contact material before the collision, m/s; v_{22}-v_{12} - the relative velocity of the seed and the contact material after the collision, m/s; h_1 - the drop height of the seed before the collision, mm; h_2 - the rebound height of the seed after the collision, mm.

As shown in Fig. 4, a high-speed imaging system was established to measure the coefficient of restitution. The system consisted of a high-speed camera, a lighting system, a self-designed drop frame, a background board, and a scale. The drop frame allowed vertical adjustment of the release height within a range of 0–50 cm.

During the test, seeds were released from predetermined heights of 10, 20, and 30 cm and allowed to freely fall onto the contact material. The rebound motion was recorded, and only trials with approximately vertical rebound were considered valid. The maximum rebound height was obtained from the recorded images using the coordinate scale. Each test was repeated five times, and the average value was used.

Fig. 4 - High-speed imaging system for restitution coefficient measurement

1. background board; 2. drop platform; 3. scale; 4. contact material; 5. drop frame; 6. lighting system; 7. high-speed camera

To evaluate the effects of seed type, moisture content, and drop height on the coefficient of restitution, experiments were conducted using millet, broomcorn millet, and rapeseed at moisture contents of 15%, 20%, and 25%. The corresponding experimental factors, levels and results are presented in Table 4. The coefficient of restitution was measured under different combinations of seed type, moisture level, and contact material.

Table 4

Experimental factors and levels and results for restitution coefficient tests

Seed type	Moisture content [%]	Drop height [cm]	Millet board	Broomcorn millet board	Rapeseed board	Acrylic board	Stainless steel board	Resin material board
Millet	15	10	0.4780	-	-	0.5868	0.5805	0.5317
		20	0.4609	-	-	0.5349	0.5314	0.4913
		30	0.4404		-	0.5107	0.5072	0.4697
	20	10	0.4657	-	-	0.5665	0.5658	0.4990
		20	0.4400	-	-	0.5214	0.5079	0.4990
		30	0.4195	-	-	0.4936	0.4907	0.4797
	25	10	0.4508	-	-	0.5538	0.5453	0.5021
		20	0.4356	-	-	0.5102	0.5106	0.4875
		30	0.4011	-	-	0.4968	0.4927	0.4608
Broomcorn millet	15	10	-	0.5376	-	0.6315	0.6281	0.5876
		20	-	0.4975	-	0.6158	0.6032	0.5600
		30	-	0.4750	-	0.5721	0.5713	0.5269
	20	10	-	0.5140	-	0.6054	0.5824	0.5680
		20	-	0.4998	-	0.5740	0.5730	0.5357
		30	-	0.4692	-	0.5370	0.5342	0.5072
	25	10	-	0.5091	-	0.5901	0.5772	0.5584
		20	-	0.4968	-	0.5607	0.5523	0.5325
		30	-	0.4707	-	0.5321	0.5316	0.5017
Rapeseed	15	10	-	-	0.4545	0.5617	0.5583	0.5375
		20	-	-	0.4276	0.5360	0.5324	0.5009
		30	-	-	0.4084	0.5115	0.5065	0.4807
	20	10	-	-	0.4287	0.5317	0.5315	0.5002
		20	-	-	0.4040	0.5046	0.5023	0.4772
		30	-	-	0.3892	0.4793	0.4721	0.4496
	25	10	-	-	0.4120	0.5276	0.5215	0.4891
		20	-	-	0.4033	0.5108	0.5017	0.4602
		30	-	-	0.3858	0.4718	0.4683	0.4540

As shown in Fig. 5, image processing was performed after the experiments. The high-speed camera operated at 300 frames per second (fps). The rebound trajectories were analyzed using i-SPEED Control Software to determine the maximum rebound height for each trial. These values were then substituted into Equation (10) to calculate the coefficient of restitution.

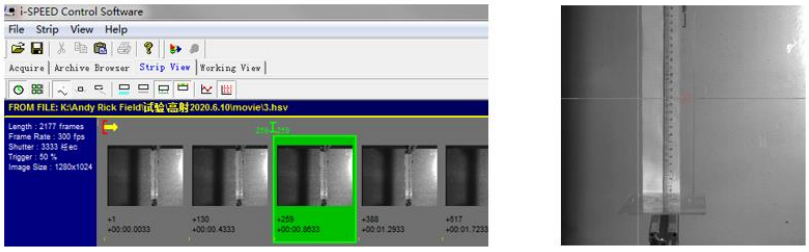

(a) (b)

Fig. 5 - Data acquisition and processing of rebound motion

(a) Image post-processing; (b) Determination of rebound height

RESULTS AND DISCUSSION

Measurement results of basic parameters

The measured basic physical parameters of the seeds are presented in Table 5. The thousand-seed weight of millet, broomcorn millet, and rapeseed was positively correlated with seed size. Among the three seed types, rapeseed exhibited the highest density, followed by millet and broomcorn millet. The moisture content of all seeds ranged from 10% to 15%. Within this range, relatively higher moisture content is generally favorable for seed germination and field establishment. These parameters provide a fundamental basis for the design and performance optimization of the seed metering device.

Table 5

Basic physical parameters of small-seed crops

Item	Millet	Broomcorn millet	Rapeseed
Moisture content [%]	11.21±0.51	14.39±1.03	12.65±0.86
Thousand-grain weight [g]	2.689±0.092	8.307±0.177	3.771±0.119
Density [kg/m³]	1015.6±15.7	907.7±16.5	1132.5±13.2
Three-axis dimensions [mm]	1.757, 1.539, 1.435	2.989, 2.465, 1.945	2.236, 2.045, 1.726
Equivalent diameter [mm]	1.5717±0.3118	2.5290±0.2756	2.1331±0.2263
Angle of repose [°]	23.80±1.37	21.19±1.65	21.89±1.87
Poisson's ratio	0.27±0.01	0.33±0.02	0.29±0.01

Results of static and kinetic friction coefficients

As shown in Fig. 6, the static and kinetic friction coefficients of millet, broomcorn millet, and rapeseed on different contact materials (acrylic, stainless steel, and resin) are presented. The results indicate that the friction coefficients were strongly influenced by the surface characteristics of the contact materials. These results are consistent with the general tribological behavior of granular materials.

In general, materials with higher surface roughness exhibited higher friction coefficients. Among the tested materials, stainless steel showed the lowest friction coefficients, followed by acrylic and resin.

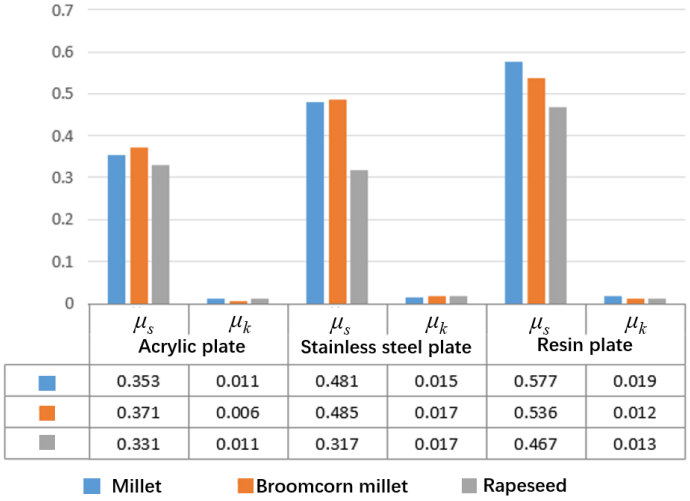

Fig. 6 - Friction coefficients of seeds on different contact materials

For a given material, the friction coefficient was also affected by seed surface characteristics. Seeds with smoother surfaces tended to exhibit lower static friction coefficients. Accordingly, the friction coefficients increased in the order of broomcorn millet, rapeseed, and millet, reflecting differences in surface texture.

In addition, seed mass had a certain influence on the kinetic friction behavior. Under similar shape conditions, heavier seeds tended to exhibit slightly lower kinetic friction coefficients, which may be attributed to increased normal force and reduced relative resistance during motion.

Elastic modulus test results

As shown in Fig. 7, the elastic modulus values of millet, broomcorn millet, and rapeseed are presented. The average elastic moduli were 351.76 MPa for millet, 589.14 MPa for broomcorn millet, and 133.37 MPa for rapeseed, indicating clear differences among the three seed types. Among them, broomcorn millet exhibited the highest elastic modulus, followed by millet and rapeseed. These results suggest that broomcorn millet exhibits greater resistance to elastic deformation compared with the other two seed types. This variation may be attributed to differences in seed internal structure and density. According to Equation (9), the shear moduli of millet, broomcorn millet, and rapeseed were 140.70 MPa, 235.66 MPa, and 53.35 MPa, respectively. This indicates that the shear resistance ranked, from strongest to weakest, as broomcorn millet, millet, and rapeseed.

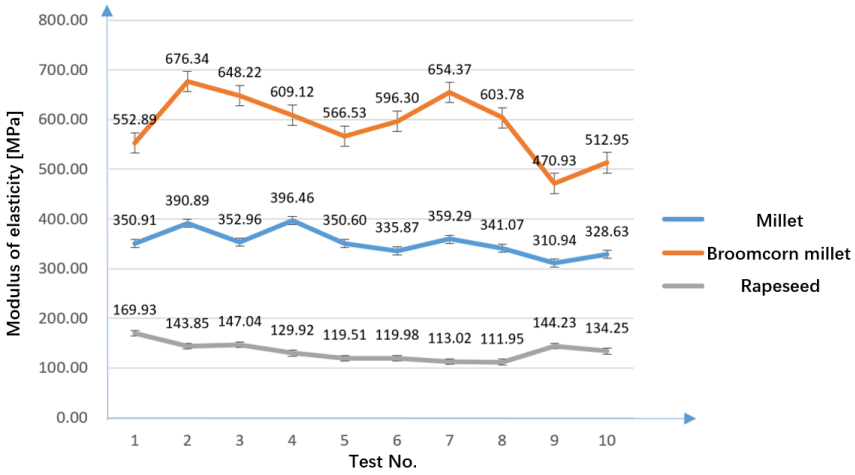

Fig. 7 - Elastic modulus of seeds

Test results of coefficient of restitution

As shown in Fig. 8, the experimental study on the collision restitution coefficients of different seed types and moisture contents with various materials leads to the following conclusions: under the same conditions, as the height increases, the collision restitution coefficient of the seeds decreases. The collision restitution coefficient is significantly related to moisture content, rapidly decreasing with an increase in moisture content. The collision restitution coefficients of broomcorn millet, millet, and rapeseed decrease in this order. Furthermore, the collision restitution coefficients between each type of seed and acrylic, stainless steel, and resin plates, as well as between seeds of the same type, decrease in the same sequence, with coefficients between acrylic and stainless steel plates being quite similar. The research on the collision restitution coefficient of small-seed crops provides important theoretical support for the design and simulation of precision seed metering devices. This trend can be attributed to increased energy dissipation during impact at higher moisture contents.

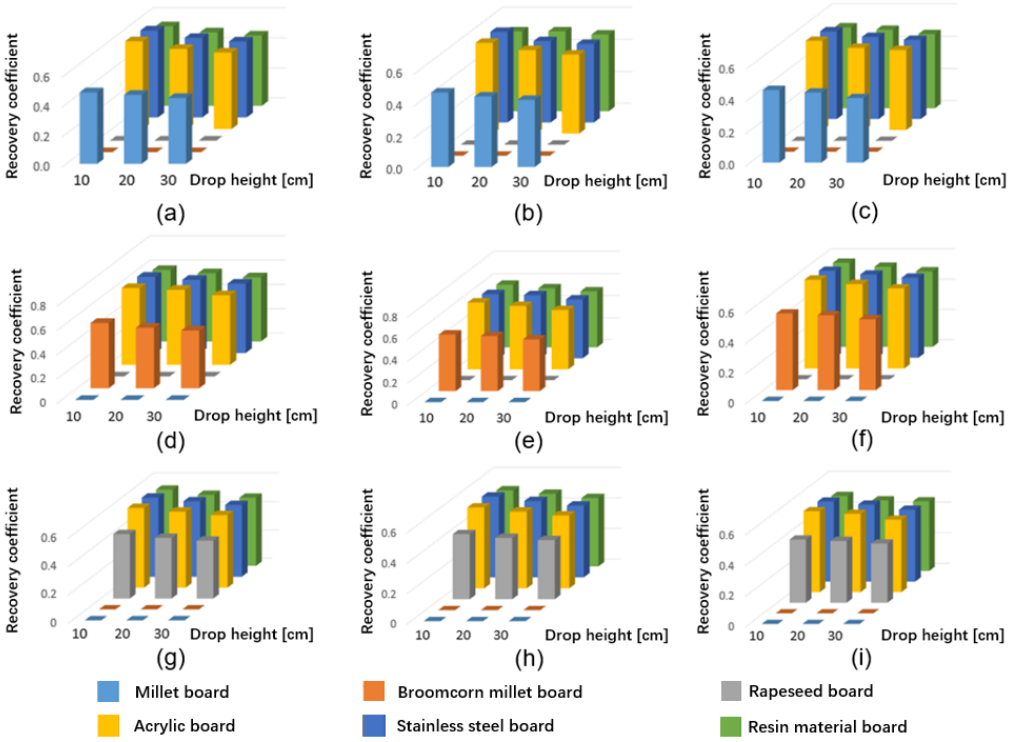

Fig. 8 - Coefficient of restitution of seeds

(a) The coefficient of restitution of millet with 15% moisture content; (b) The coefficient of restitution of millet with 20% moisture content; (c) The coefficient of restitution of millet with 25% moisture content; (d) The coefficient of restitution of broomcorn millet with 15% moisture content; (e) The coefficient of restitution of broomcorn millet with 20% moisture content; (f) The coefficient of restitution of broomcorn millet with 25% moisture content; (g) The coefficient of restitution of rapeseed with 15% moisture content; (h) The coefficient of restitution of rapeseed with 20% moisture content; (i) The coefficient of restitution of rapeseed with 25% moisture content

CONCLUSIONS

This study determined the key physical and mechanical characteristics of millet, broomcorn millet, and rapeseed to support the design and simulation of pneumatic precision seed metering devices for small-seed crops. The main conclusions are as follows:

(1) The three seed types showed clear differences in basic physical characteristics. Their equivalent diameters were 1.5717, 2.5290, and 2.1331 mm, and their densities were 1015.6, 907.7, and 1132.5 kg/m³, respectively. These differences indicate that crop-specific parameters should be used in seed metering design and simulation.

(2) Friction characteristics varied significantly with contact material. In general, friction coefficients were lowest on stainless steel, followed by acrylic and resin, indicating that material selection directly affects seed flow and filling stability.

(3) The average elastic modulus values of millet, broomcorn millet, and rapeseed were 351.76, 589.14, and 133.37 MPa, respectively. This shows that different small-seed crops have distinct deformation and contact-response behaviors and should not share the same mechanical parameters in simulation.

(4) The coefficient of restitution decreased with increasing drop height and moisture content, indicating that seed collision behavior is sensitive to operating conditions and should be considered in seed-motion analysis.

(5) The parameter dataset obtained in this study provides basic support for material selection, structural optimization, suction-stability analysis, and numerical simulation of pneumatic precision seed metering devices for small-seed crops.

ACKNOWLEDGEMENT

This study was supported by the National Natural Science Foundation of China (32272001), the Shaanxi Key Research and Development Project (2023-ZDLNY-62), and the Shaanxi Key Research and Development Project (grant number 2022NY-205).

REFERENCES

[1] Dun G., Wang L., Xue H., Ji X., Sheng Q., Li X., Zhang C., & Wei Y. (2025). Statistics and analysis of physical parameters of adzuki bean seeds. *INMATEH Agricultural Engineering*, 76(2), 433-446. https://doi.org/10.35633/inmateh-75-37

[2] Hu H., Zhou Z., Wu W., Yang W., Li T., Chang C., Ren W., & Lei X. (2021). Distribution characteristics and parameter optimisation of an air-assisted centralised seed-metering device for rapeseed using a CFD-DEM coupled simulation. *Biosystems Engineering*, 208, 246-259. https://doi.org/10.1016/j.biosystemseng.2021.06.005

[3] Ibrahim, E. J., Liao, Q., Wang, L., Liao, Y., & Yao, L. (2018). Design and experiment of multi-row pneumatic precision metering device for rapeseed. *International Journal of Agricultural and Biological Engineering*, 11(5), 116–123. https://doi.org/10.25165/j.ijabe.20181105.3544

[4] Jin, X., Li, Q., Zhao, K., Zhao, B., He, Z., & Qiu, Z. (2019). Development and test of an electric precision seeder for small-size vegetable seeds. *International Journal of Agricultural and Biological Engineering*, 12(2), 75–81. https://doi.org/10.25165/j.ijabe.20191202.4618

[5] Karayel, D. (2009). Performance of a modified precision vacuum seeder for no-till sowing of maize and soybean. *Soil and Tillage Research*, 104(1): 121-125. https://doi.org/10.1016/j.still.2009.02.001.

[6] Karayel, D., Barut, Z.B., & Ozmerzi, A. (2004). Mathematical modelling of vacuum pressure on a precision seeder. *Biosystems Engineering*, 87(4): 437-444. https://doi.org/10.1016/j.biosystemseng.2004.01.011.

[7] Lai, Q., Sun, K., Yu, Q., & Qin, W. (2020). Design and experiment of a six-row air-blowing centralized precision seed-metering device for Panax notoginseng. *International Journal of Agricultural and Biological Engineering*, 13(2), 111–122. https://doi.org/10.25165/j.ijabe.20201302.5161

[8] Lei X., Hu H., Wu W., Liu H., Liu L., Yang W., Zhou Z., & Ren W. (2021). Seed motion characteristics and seeding performance of a centralised seed metering system for rapeseed investigated by DEM simulation and bench testing. *Biosystems Engineering*, 203, 22-33. https://doi.org/10.1016/j.biosystemseng.2020.12.017

[9] Li H., Liu S., Wu G., Yan B., & Ling L. (2025). Methods and experimental study on the determination of friction and mechanical property parameters of various rice seed varieties under different conditions. *INMATEH Agricultural Engineering*, 76(2), 416-427. https://doi.org/10.35633/inmateh-76-35

[10] Li H., Yan B., Meng Z., Ling L., Yin Y., Zhang A., Zhao C., & Wu G. (2023a). Study on influencing factors of hole-filling performance of rice precision direct seed-metering device with hole ejection. *Biosystems Engineering*, 233, 76-92. https://doi.org/10.1016/j.biosystemseng.2023.07.006

[11] Li, Y., Bai, Y., Zhang, X., & Xie, F. (2023b). Structural design and simulation analysis of a dual-row pneumatic vegetable precision planter. *Processes*, 11(6), 1803. https://doi.org/10.3390/pr11061803

[12] Li, Z., Wu, J., Du, J., Duan, D., Zhang, T., & Chen, Y. (2023c). Experimenting and optimizing design parameters for a pneumatic hill-drop rapeseed metering device. *Agronomy*, 13(1), 141. https://doi.org/10.3390/agronomy13010141

[13] Liu, R., Liu, L., Li, Y., Liu, Z., Zhao, J., Liu, Y., & Zhang, X. (2022). Numerical simulation of seed-movement characteristics in new maize delivery device. *Agriculture*, 12(11), 1944. https://doi.org/10.3390/agriculture12111944

[14] Onal, I., Degirmencioglu, A., & Yazgi, A. (2012). An evaluation of seed spacing accuracy of a vacuum type precision metering unit based on theoretical considerations and experiments. *Turkish Journal of Agriculture and Forestry*, 36(2): 133-144. https://doi.org/10.3906/tar-1010-1316.

[15] Singh, R.C., Singh, G., & Saraswat, D.C. (2005). Optimisation of design and operational parameters of a pneumatic seed metering device for planting cottonseeds. *Biosystems Engineering*, 92(4): 429-438. https://doi.org/10.1016/j.biosystemseng.2005.07.002.

[16] St Jack, D., Hesterman, D., & Guzzomi, A. (2013). Precision metering of Santalum spicatum (Australian Sandalwood) seeds. *Biosystems Engineering*, 115(2): 171-183. https://doi.org/10.1016/j.biosystemseng.2013.03.004.

[17] Sun J., Yang Z., Guo Y., Cui Q., Wu X., & Zhang Y. (2017). Compression mechanical properties and crack formation law of millet grain (谷子籽粒压缩力学性质及损伤裂纹形成机理). *Transactions of the Chinese Society of Agricultural Engineering*, 33(18), 306-314. https://doi.org/10.11975/j.issn.1002-6819.2017.18.040

[18] Xu, J., Hou, J., Wu, W., Han, C., Wang, X., Tang, T., & Sun, S. (2022). Key structure design and experiment of air-suction vegetable seed-metering device. *Agronomy*, 12(3), 675. https://doi.org/10.3390/agronomy12030675

[19] Yang Z., Guo Y., Cui Q., & Li H. (2016). Test and influence factors analysis of friction characteristics of millet (谷子摩擦特性试验及其影响因素分析). *Transactions of the Chinese Society of Agricultural Engineering*, 32(16), 258-264. https://doi.org/10.11975/j.issn.1002-6819.2016.16.035

[20] Yazgi, A., & Degirmencioglu, A. (2007). Optimisation of the seed spacing uniformity performance of a vacuum-type precision seeder using response surface methodology. *Biosystems Engineering*, 97(3): 347-356. https://doi.org/10.1016/j.biosystemseng.2007.03.013.

[21] Yazgi, A., & Degirmencioglu, A. (2014). Measurement of seed spacing uniformity performance of a precision metering unit as function of the number of holes on vacuum plate. *Measurement*, 56: 128-135. https://doi.org/10.1016/j.measurement.2014.06.026.

[22] Yuan J., Wan X., Liao Q., Gao D., Xiao W., & Yang J. (2022). Mechanical compression characteristics of rapeseed based on continuous damage theory. *Biosystems Engineering*, 224, 301-312. https://doi.org/10.1016/j.biosystemseng.2022.10.008

[23] Zhang C., He X., Wang X., & Li Y. (2025). Structural design and simulation analysis of air-absorbing vegetable precision seeder. *INMATEH Agricultural Engineering*, 7(1), 190-199. https://doi.org/10.35633/inmateh-75-16